

# De-ghosting for Image Stitching with Automatic Content-awareness

Yu Tang, Jungpil Shin

Graduate School of Computer Science and Engineering  
The University of Aizu  
Aizuwakamatsu, Fukushima-ken, Japan  
{m5132108,jpshin}@u-aizu.ac.jp

**Abstract**—Ghosting artifact in the field of image stitching is a common problem and the elimination of it is not an easy task. In this paper, we propose an intuitive technique according to a stitching line based on a novel energy map which is essentially a combination of gradient map which indicates the presence of structures and prominence map which determines the attractiveness of a region. We consider a region is of significance only if it is both structural and attractive. Using this improved energy map, the stitching line can easily skirt around the moving objects or salient parts based on the philosophy that human eyes mostly notice only the salient features of an image. We compare result of our method to those of 4 state-of-the-art image stitching methods and it turns out that our method outperforms the 4 methods in removing ghosting artifacts.

**Keywords**- ghosting artifact;image stitching;improved energy map;prominence map

## I. INTRODUCTION

Dynamic elements in the overlap region often lead to unbearable ghosting artifacts in the field of image stitching. Although existing image studies are various and have different focuses but not many specialized in eliminating the ghosting. A tonal registration method[1] which is robust to moving, however, this works only when the presence of same moving objects in consequent frames which will not alter the overall histogram. Uyttendaele et al. [7]presents a weighted vertex cover algorithm to remove ghost effects , yet, this method is not failsave. Since the algorithm only prefers removing regions that are near the edge of the image because the vertex weights are computed by summing the feather weights in the ROD[7].Multi-blending [4,6,10] is effective for de-ghosting but not in the case of presence of so many moving objects. Stitching line method conceived in [3,5] is good but cannot always find a satisfactory stitching line. Our paper still adopts stitching line method but the distinct feature is that our method can detect the prominent objects with automatic-awareness and thus can always search out an optimal stitching line to remove ghosting with least distortion.

## II. BRIEF GENERAL SCHEME

Given two input images  $I_1, I_2$  in Fig.1(a) and (b), after registration we get an aligned image. We define the part of

Image  $I_1$  in the overlap region as  $\theta_1$ (the part of  $I_2$  as  $\theta_2$ , respectively). The subtraction between two images  $\theta_1(x, y)$  and  $\theta_2(x, y)$  in R, G, B channel, expressed as:

$$\theta^i(x, y) = \theta_1^i(x, y) - \theta_2^i(x, y), \quad i \in \{R, G, B\} \quad (1)$$

The subtracted image  $\theta$  is shown in Fig.1(f) and (i). In order to remove the ghosting effects we target on searching a stitching line in  $\theta$  which can intelligently go around the contour of the car. And stitch the two images according to this line.

## III. IMPROVED ENERGY MAP

Although [3,9,11]shows that the gradient enjoys the advantage of respecting structures within the image thanks to assigning higher value on edges, the demerit lies in the gradient magnitude can be misled by trivial and repeated structures and salient objects are not well detected. In our improved energy map, we combine it with prominence map which considers the regions that are attractive but homogeneous as salient. Based on that, an optimal stitching line can always be found out for de-ghosting.

### A. Prominence Map

1) *Tentative Detection*: To begin with, we roughly determine the prominence by evaluating the Euclidean distance of the average Lab vector value of an input image with each pixel vector value as:

$$E_{tent} = \|G_{\mu} - G(x, y)\| \quad (2)$$

where  $G(x, y)$  is the input image,  $G_{\mu}$  is the average of all Lab pixel vectors of the image,  $E_{tent(x, y)}$  is the pixel prominence at position  $(x, y)$ . We use the Lab space instead of RGB space since RGB space does not take lightness of the color into consideration. Also Lab space also has advantage of approximating human vision and aspiring to perceptual uniformity. When  $E_{tent(x, y)} > T$  (a threshold value), we impose a mark(shown as the green blocks in Fig.2(a) on that pixel which signifies that this pixel might be of importance since it keeps a large distance from the other pixels in the

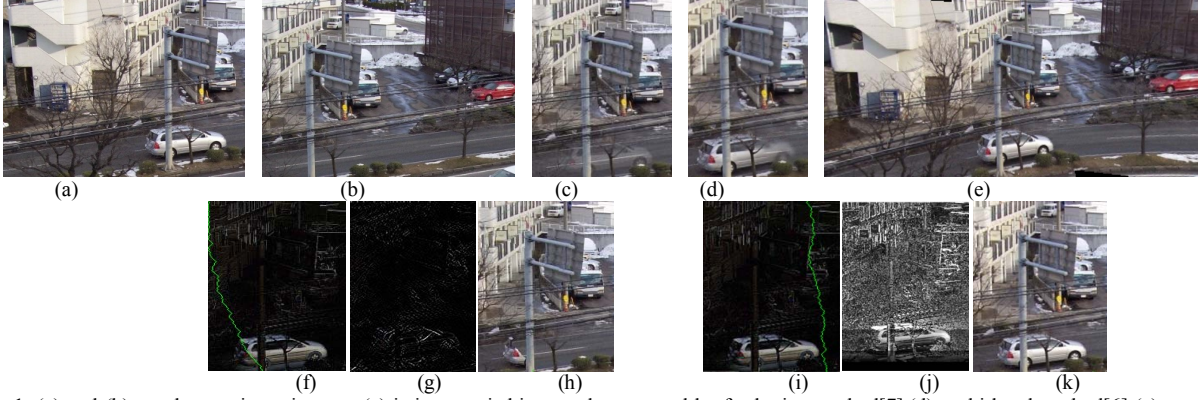


Figure 1. (a) and (b) are the two input images. (c) is image stitching result generated by feathering method[7].(d) multi-band method[6] (e) structure deformation method[2]. The orange line indicates the shape of the traffic way is bent to curve. (f) to (h) is for our previous work[3] where subtracted image (f) shows the stitching line calculated by gradient map(g) and (h) is the stitching result. (i) to (k) is for the method of this work where subtracted image (i) shows the stitching line calculated by improved energy map(j) and (k) is the stitching result. Our result(k) shows the best.

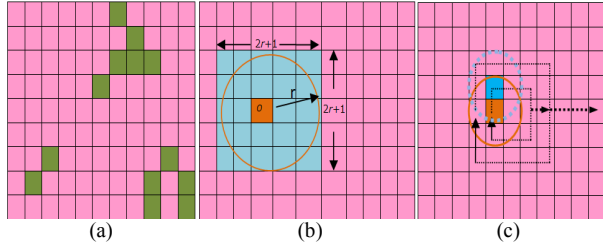


Figure 2. (a) Tentative detection based on global contrast. (b) The prominence detection based on local contrast of an image region with respect to its neighborhood is defined within a circle of radius  $r$ . (c) Filtering the images at one of the scales in rotate-expanding manner.

whole image. So in this stage, the prominent pixels are only tentatively identified.

2) *Circular Scanning*: Last stage, the tentative detection is based on the global contrast of the image. In this stage, we determine the prominent pixels on the basis of the local contrast of an image region with respect to its neighborhood. Thereby, we define a pixel as origin  $O(x, y)$  and designate its neighborhood as a circular region with radius  $r$  around it shown as Fig2.(b). The orange block is the origin  $O(x, y)$  while the blue blocks enclosed or passed by the orange circle are the neighborhood of origin  $O$ . The neighborhood is  $(2r+1) \times (2r+1)$  block region in practical terms. The prominence of the origin  $O$  is evaluated as:

$$E_{pro}^i(O) = \|N_{\mu}^r - v(O)\|, \quad i \in \{1,2,3\} \quad (3)$$

where  $N_{\mu}^r$  represents the mean vector value of the neighboring pixels within the circular region with radius  $r$  in Lab space while  $v(O)$  denotes the vector value of origin.  $E_{pro}^i(O)$  is still the  $L_2$ -norm measured by Euclidean distance. Parameter  $i$  indicates that the prominence of the pixel is in which scale. We will calculate the prominence at three scales in total.  $N_{\mu}^r$  is simply computed as :

$$N_{\mu}^r = \frac{1}{N} \sum_{n=1}^N v_n \quad (4)$$

where  $N$  is the total pixels of the neighborhood. The filtering is performed in a rotate-expanding manner as Fig.2(c) shown. The origin of the circle first rotates around the innermost region in the direction of the innermost arrowed line. In the following procedure, the new orbit will expand outward by one pixel every time. In the process of searching, the pixels which are marked as potentially-prominent may be covered by the circular filter from time to time. The Equation (4) will be altered as :

$$N_{\mu}^r = \frac{1}{N} \sum_{n=1}^N (v_n^k + kw v_n^k), \quad k \in \{0,1\} \quad (5)$$

When  $k=1$ ,  $v_n^k$  denotes the potentially-prominent pixel identified in the tentative detection stage. The additional weight  $w(w=0.1$  in this paper) will be attached to it.

3) *Prominence Summation and Stitching Line Searching*: For an input image of width  $w$  and height  $h$  pixels, the radius  $r$  of the circular filter is varied as:  $\frac{w}{16} \leq r \leq \frac{w}{4}$ . Suppose  $w$  to be smaller than  $h$  (else we choose  $h$  to decide radius). One observation merit attention is that radius larger than  $\frac{w}{4}$  of the filter cannot identify small salient objects or smaller than  $\frac{w}{16}$  highlighted the petty objects in an excessively finer manner. In our work, we perform filtering at three different scales with radius of  $\frac{w}{4}, \frac{w}{8}, \frac{w}{16}$ . Finally we get the prominence map  $G_{prom}$  obtained by point-wise summation of prominence values at three scales:

$$G_{prom}(x, y) = \sum_{i=1}^3 E_{pro}^i(x, y) \quad (6)$$

where  $x \in [1, w], y \in [1, h]$ . Since our previous work[3] shows the satisfactory stitching results based on the gradient energy map as:

$$G_{grad}(x, y) = \left| \frac{\partial}{\partial x} G \right| + \left| \frac{\partial}{\partial y} G \right| \quad (7)$$

Our improved energy map also takes gradient values into consideration for respecting structural information of the original image as:

$$G_{imp}(x, y) = G_{grad}(x, y) + G_{prom}(x, y) \quad (8)$$

The improved energy map is virtually a summation of the corresponding pixel-wise gradient value and prominent value. Since less energy more unnoticeable, we aim at finding a low energy path as our stitching line. We adopt the Greedy Searching Algorithm [3] in order to reduce the computational cost.

### B. Comparison and Analysis

As shown in Fig. 3 column (a), given an original image (first row) and its Gaussian twice-blurred version (using  $3 \times 3$  binomial kernel) in the second row. We explore the stitching lines within prominence map, gradient map, improved energy map and in the column (b)(c)(d), respectively. It is obvious that prominence map and improved energy map protect the whole body of geisha against the passing of stitching lines very well. What is more, the two maps verify their robustness to the very noise. In contrast, the gradient map shows far worse results in the two versions since the stitching lines are either clustered to one side or just cross the body of geisha.

Let us identify the reason for gradient map's failure of protecting the salient objects by comparing the profiles of the three maps in both local and global manner as Fig. 4. First, the colored energy maps of prominence map and improved energy map present that quite a bit of pixels with high visual significance (prominent pixels are marked in red) are distributed in the region of geisha evenly, while gradient map only assigns visual importance to the edges or trivial structures. In other words, the amount of significant pixels is too few to protect the salient object. Assuming our stitching lines are horizontal or vertical straight lines as shown in the colored energy map. The top and right line charts showing the value of each pixel of the corresponding position in the horizontal and vertical stitching lines, respectively. Apparently the energy of stitching lines in the prominence map and improved energy map are much higher and more uniform than that in the gradient map.

To fix the intractable problem of ghosting, safeguarding single salient object is far insufficient, our improved energy map is also very effective for protecting multi-objects as shown in Fig.5.

## IV. EXPERIMENTAL RESULTS

We demonstrate our method capable of generating natural image stitching results for presence of either single moving object or multi-moving-objects. Comparison with

other methods is also given.

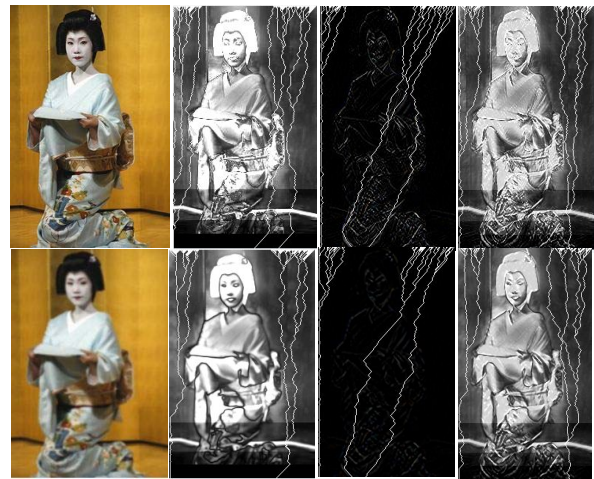


Figure 3. Column (a) shows original (above) and noise version (below) of the image. Column (b)(c)(d) shows several less energy stitching lines calculated on prominence map, gradient map, improved energy map.

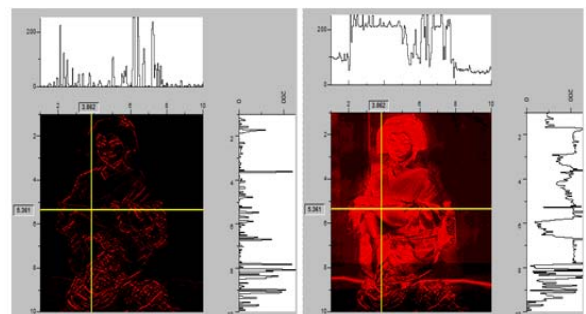


Figure 4. Profiles of gradient map and improved energy map from Left to right.



Figure 5. Column (a) and (c) shows original images with less energy stitching lines calculated by corresponding improved energy maps and gradient maps in Column (b) and (d), respectively.

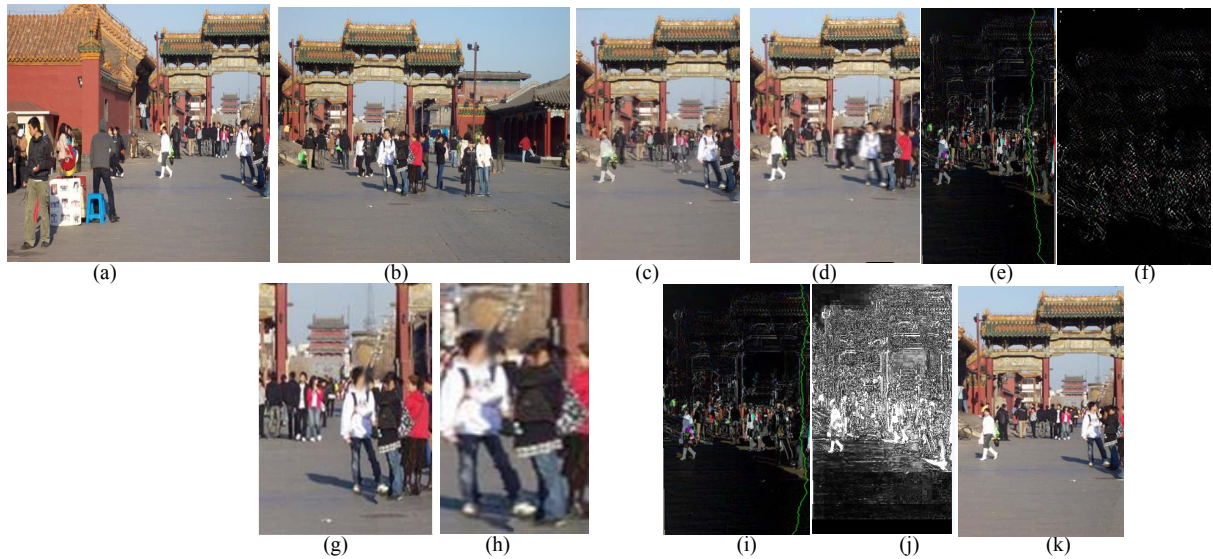


Figure 6. (a)(b) two input images. (c) image stitching result generated by tonal registration [1] (d) multi-band method[6]. (e) to (h) is for our previous work[3] where subtracted image (e) shows the stitching line calculated by gradient map(f) and (g) is the stitching result. (h) is the enlarged view of (g). (i) to (k) is for the method of this work where subtracted image (i) shows the stitching line calculated by improved energy map(j) and (k) is the stitching result. Our result(k) shows the best.

In, Fig.1, (a) and (b) show two overlapped images of an automobile ambulation scene. Ghosting artifact is obvious in (c) using the Feathering algorithm[7]. (d) use the multi-blend algorithm and presents a much better result than (c). Nevertheless, apparent blurring displays in the vicinity of car's head. At first sight, (e) is a good stitched mosaic, however, it is not a true reflection of input pictures since the original straight shape of the motor way is bent to a curve due to the deformation method in [2]. (h) is the result of [3] based on gradient map. Due to the stitching line's failure of avoiding the prominent object, a small fraction of car is remained. (k) shows the best result using our improved energy map(j) and stitching line(i).

Notice that many moving objects are contained in the scene in Fig.6, it could be a very difficult and challenging sequence. (c), (d) are generated by [1] and [6] and display ghosting artifacts and fuzzy effect, respectively. (g) shows the result using stitching line in (e) searched by method[3] with gradient energy map (f). Since the stitching line passes through the man's face, the distortion of the man's face is clearly observed in enlarged view of (g) in Fig.(h). Finally, please note how the stitching line avoid people in (i) based on our improved energy map(j) and obtain the satisfactory result in (j) and it shows the best.

## V. CONCLUSION

In this work, to eliminate ghosting artifacts, we present a novel energy map for finding an optimal stitching line which is automatically aware of the content and thus skirts around the salient objects. Since the energy map is essentially a combination of gradient map and prominence map which assigns higher importance to whole visually

prominent regions(not only edges), the stitching line can easily skirt around the moving objects. The result section demonstrates that our method is better than the other four state-of-the-art[1,2,3,6] techniques for de-ghosting.

## REFERENCES

- [1] P.Azzari and A.Bevilacqua. Joint spatial and tonal mosaic alignment for motion. Proceeding on AVSS 2006, pp.89-102, Nov. 2006.
- [2] Jia jia, Chi-Keung Tang. Image stitching using structure deformation. Pattern Analysis and Machine Intelligence IEEE Transactions. 30(4):617-631, Apr. 2008.
- [3] Yu Tang, Huiyan Jiang. Highly efficient image stitching based on energy map. CISP'09, pp.1-5, Oct. 2009.
- [4] Allene, C, Pons,J. Seamless image-based texture atlases using multi band blending. ICPR 2008, pp.1-4, Dec,2008
- [5] Han,B, Lin,X. A novel hybrid color registration algorithm for image stitching. Consumer Electronics, IEEE Transactions, 52(3):1129-1134, Aug. 2006
- [6] M.Brown, D.G. Lowe. Automatic panoramic image stitching using invariant features. International Journal of Computer Vision, Pp. 59-73, August. 2007
- [7] M.Uyttendaele, A.Eden. Eliminating ghosting and exposure artifacts in image mosaics. CVPR2001, pp.509-516, Dec.2001.
- [8] Tien-Der Yeh, Yon-Ping Che. An image stitching process using band-type optimal partition method. Asian Journal of Information Technology, 7(11):498-509, 2008.
- [9] Xiong, Yingen. Eliminating ghosting artifacts for panoramic images. ISM'09 pp: 14-16, Dec. 2009
- [10] [Li Yao. Image mosaic on SIFT and deformation propagation. Knowledge Acquisition and Modeling Workshop, 2008, pp: 848-851, Dec. 2008.
- [11] Anat Levin, Assaf Zomet. Seamless image stitching in the gradient Domain. ECCV 2004, pp:377-389,May.2004